

Optical Constants Determination of Thermally-Evaporated Undoped Lead Iodide Films from Transmission Spectra Using the PUMA Method

Mahmoud H. Saleh

Department of Physics, Faculty of Science, Al-Balqa Applied University, Al-Salt 19117, Jordan.

Received on: 9/5/2018;

Accepted on: 24/6/2018

Abstract: 0.7- μm thick lead iodide (PbI_2) films thermally-evaporated on glass substrates held at different temperatures T_s (35 – 195 °C) are studied. Typical observed X-ray diffraction (XRD) patterns and scanning electron microscope (SEM) micrographs of such PbI_2 films prepared at high substrate temperatures T_s (> 100 °C) were found to be crystalline with hexagonal 2H-polytypic structure with the c -axis perpendicular to the surface. The room-temperature normal-incidence transmittance $T_{\text{exp}}(\lambda)$ of the PbI_2 films has been measured as a function of spectral wavelength λ in the range 300 – 1100 nm and was used to retrieve the spectral dependence of their optical constants $n(\lambda)$ and $\kappa(\lambda)$ using the Pointwise Unconstrained Minimization Approach (PUMA) method. The energy variation of the absorption coefficient $\alpha(\lambda) (= 4\pi\kappa(\lambda)/\lambda)$ of the PbI_2 films in the region of strong optical absorption was analyzed using various interband transition models and was found to be reasonably described by an approximate power-law relation $ahv \propto (hv - E)^m$, with $m = 2$ and $E_g^{\text{opt}} \cong 2.2$ eV ($\pm 2\%$) (Tauc interband dielectric model, where E_g^{opt} is the optical bandgap energy). But, it is more remarkable for $m = 1/2$ and $E_g \cong 2.45$ eV ($\pm 2\%$) (direct interband transition model) over a broader spectral range. For $T_s > 100$ °C and in the transparent and weak absorption regions, the PUMA-retrieved $n(\lambda) - \lambda$ data of the PbI_2 films was found to fit the Wemple-DiDomenico (WDD) dispersion formula, with bandgap energy parameter $E_o \cong 3.9$ eV $\cong 2 E_g^{\text{opt}}$, single-oscillator energy strength $E_d \cong 19$ eV and static index of refraction $n_o \cong 2.5$. Analysis of the data in the absorption tail to Urbach formula yielded an Urbach-tail parameter Γ_U that decreased with increasing substrate temperature to a value around 75 meV at the high substrate temperature side. These results indicate that using film growth temperatures beyond 100 °C leads to an enhancement in the crystallinity of the PbI_2 films and reduces band tailing.

Keywords: PbI_2 films, Optical constants, PUMA method, Wemple-DiDomenico model, Interband transition models.

Introduction

Lead iodide (PbI_2) is considered an attractive material in the fabrication of many technological devices, such as photocells and room-temperature (RT) crystalline radiation detectors and X-ray diagnostic imaging systems for detecting low and intermediate energy X- and γ -rays (1 keV – 1 MeV), as PbI_2 can efficiently

operate over a wide temperature range ($-200^\circ\text{C} - 130^\circ\text{C}$) [1, 6]. This is because purely crystalline PbI_2 is a direct band-gap p-type compound semiconductor with large band gap energy E_g of (~ 2.5 eV) and high dark dc resistivity ($\rho \sim 10^{13} \Omega \cdot \text{m}$ at 300K) [2-8]; thus giving rise to low-noise and low leakage current in devices incorporating it [2-4]. Moreover, lead

iodide requires rather small energy for the creation of an electron-hole pair ($E_{e-h} \sim 5 - 6.6$ eV); thus producing many charge carriers with high signal-to-noise electrical response [2, 5, 6]. Lead iodide possesses several other advantageous physical properties; for example, PbI_2 has a high melting point (~ 405 °C), high quantum efficiency [4-8], high mass density (6.2 g/cm³) and is composed of elements of large atomic numbers ($Z_{\text{Pb}} = 82$ and $Z_{\text{I}} = 53$); hence exhibiting high photon stopping power (due to its high atomic absorption coefficient $\sim 10^5$ cm⁻¹) [5-12]. These features are supposed to render lead iodide to be structurally stable and efficient in a variety of room-temperature electronic devices incorporating crystals and polycrystalline layers (films) designed from this material.

However, despite the rich literature work spent on lead iodide crystals and films, some important physical properties demand more attention and detailed investigation of their optical constants and bandgap structure. In fact, determination of optical parameters of semiconducting samples, such as polycrystalline PbI_2 films from data of optical spectroscopic measurements made on film-substrate structure, is not a simple task and requires rigorous and sophisticated analytical and computational tools [13-19]. Several methods have been used for analyzing optical transmittance spectra of four-layered optical film substrate of the (air/film/substrate/air) configuration, such as conventional-iterative curve fitting programs [13], algebraic Swanepoel envelope method [14-16] and Pointwise Unconstrained Minimization Approach (PUMA) method [17-19]. Regarding lead iodide films, no literature studies have been carried out of their optical transmittance (or reflectance) spectra by the numeric PUMA method [17-19], which does not require, as the Swanepoel envelope method, the use of dielectric dispersion relations for the optical constant of studied films, but retrieves them as an output of its numeric analysis [14, 15].

In the present work, the numeric PUMA method will be adopted to analyze measured normal-incidence transmittance $T_{\text{exp}}(\lambda) - \lambda$ data of {air/ PbI_2 film/thick glass slide/air}-samples. One of the usual algebraic methods is the Swanepoel envelope method, which is usable if the measured transmittance spectrum displays many maxima and minima fringes in the optically transparent and weakly-absorbing

regions of its film and substrate [14, 15]. The numeric PUMA method does not need any dispersion relations a priori or the number of interference maxima and minima fringes on the $T_{\text{exp}}(\lambda)$ spectra to exploit the effectiveness of this method for analyzing optical spectra of multi-layered structures and use its output results to acquire more insight into spectral dispersion of the dielectric and optical functions of PbI_2 films. [17-19]. Further, most of publications on thin PbI_2 films are concerned with the analysis of experimental transmission spectra based on basic traditional calculations [20-29].

Experimental Details

Conventional vacuum thermal evaporation was used to prepare lead iodide thin films on glass slides from commercial lead iodide powder (BDH, England) that was ground into fine powder, which was purified to get crystal chunks. The purified lead iodide powder was then placed in a molybdenum crucible situated below the substrates inside the vacuum chamber of a Leybold deposition system (LEYBOLD-HERAEUS UNIVEX 300) which was pumped down to pressure around 10^{-5} mbar. The glass substrates located 15 cm above the crucible were maintained at a constant temperature T_s in the range (35 – 195 °C). In each deposition run, a batch of lead iodide films of geometric thickness d around 0.7 μm , as recorded by an INFICON-XTC quartz crystal monitor unit, were produced at low evaporation rates (10 – 20 Å/s). Table 1 shows labelling of the studied thermally-evaporated lead iodide films prepared at different substrate temperatures T_s . The structure and surface morphology of these lead iodide films were then characterized by room-temperature X-ray diffraction (XRD) (SHIMADZU XRD-7000 diffractometer), scanning electron microscopy (SEM) (Inspect F50 model Eindhoven) and energy dispersive X-ray analysis (EDAX) detector (Bruker Microanalysis GmbH).

TABLE 1. Preparation conditions of lead iodide films prepared by the thermal-evaporation technique.

Sample label	Substrate temperature T_s (°C)
S35	35
S95	95
S125	125
S160	160
S195	195

The specular transmittance values of a typical 1.1-mm thick glass slide standing freely in air and of the (PbI₂-film/glass substrate) samples were measured at room temperature as a function of wavelength λ of collimated light incident normally at the air-film interface using a conventional double-beam UV-VIS-NIR spectrophotometer (SHIMADZU UV-1800). All normal-incidence transmittance measurements were taken relative to air-baseline transmission normalized to 100%, with the sample being placed in the path of a spectrophotometer light beam and the reference-beam path always left open. The wavelength was scanned in the range 300 – 1100 nm at a rate of 120 nm/min and 0.5 nm-interval, with 0.5 nm spectral bandwidth (SBW) of the incident light beam to minimize the SBW effect on the shape and features of transmittance spectra of the studied PbI₂/glass-substrate samples.

Results and Discussion

Structure of Evaporated Lead Iodide Films

Lead iodide films produced from purified lead iodide crystalline chunks by thermal evaporation on glass slides held at high substrate temperatures were found to be preferentially crystalline in the 2H-polytype hexagonal structure along the *c*-axis, alongside the (00*l*) lattice orientation directions. These findings are clearly revealed from their measured X-ray diffraction (XRD) patterns and scanning electron microscope (SEM) micrographs as shown in Fig. 1 a and b for a typical 0.7- μ m thick lead iodide film prepared at substrate temperatures T_s (35 and 160 °C). The lead iodide films were polycrystalline at low substrate temperatures ($T_s < 100$ °C). However, increasing T_s above 100 °C, the 2H-polytype hexagonal structure of lead iodide films has been largely enhanced, where the polycrystallinity features diminished and the films became preferably crystalline along the *c*-axis of hexagonal structure. These features are noted from their measured XRD patterns and SEM micrographs and agree with previous studies prepared PbI₂ films by thermal-evaporation [30], but different from PbI₂ films prepared by flash-evaporation method [21, 31]. Microscopic visualization showed that the deposited PbI₂ films were free from pin holes and cracks; their SEM micrographs manifested smooth and homogeneous surfaces.

The XRD patterns and SEM micrographs of the lead iodide films that were prepared at $T_s > 100$ °C are similar to those reported in the literature for PbI₂ films prepared by conventional thermal evaporation at high substrate temperatures [12, 25, 30] and with those found for PbI₂ films prepared by flash evaporation [21, 31], by physical vapor deposition similar to those used in the present work (PVD) [23, 32, 33] and to some extent with those XRD results reported for lead iodide films prepared by the chemical dipping method [24]. However, the obtained XRD patterns and SEM micrographs of thermally prepared lead iodide films in the present work are inconsistent with the good results for polycrystalline PbI₂ films prepared by spray pyrolysis [20], spin coating [26] and conventional thermal evaporation at low substrate temperatures [22, 28, 30].

The energy dispersive spectroscopy (EDS) measurements on evaporated PbI₂ films showed that these films were nearly stoichiometric with PbI_(0.7-1.45)-composition-dependending T_s . The EDS results of evaporated lead iodide films in the present work are better than the EDS compositions reported for lead iodide films prepared by the spray pyrolysis method [20] and by the chemical dipping method [24].

Normal-Incidence Optical Transmittance Spectra of {Lead Iodide/Glass-Substrate} Samples

In measuring normal-incidence transmission of {air/PbI₂ film/glass slide/air}-samples, monochromatic light beams with reasonably small SBWs (≤ 2 nm) were used, so the effect of slit width on their $T_{\text{exp}}(\lambda) - \lambda$ spectra is not significant [14]. Typical room-temperature $T_{\text{exp}}(\lambda) - \lambda$ spectra of these samples at different substrate temperatures (35-195 °C) are shown in Fig. 2, which shows some prominent features that can be useful in their forthcoming optical analysis.

For PbI₂ films prepared at low T_s , the decrease of transmittance in the absorption-edge is not steep, but exhibits a monotonic gradual decrease with wavelength, suggesting that the crystallinity of these films is not as good as that of films prepared at high T_s ; a feature that can be due to lattice disorder and non-stoichiometric defects present in them. It is noticed from Fig. 2 that the $T_{\text{exp}}(\lambda)$ curve of the 0.7- μ m thick PbI₂ films prepared at high substrate temperatures T_s

(>100 °C) clearly illustrates a sharp fundamental absorption-edge near the spectral wavelength $\lambda \approx 520$ nm [21, 30-32]. This indicates that this

film is crystalline and is in good agreement with the XRD and SEM results observed for our films at high T_s (see Fig. 1).

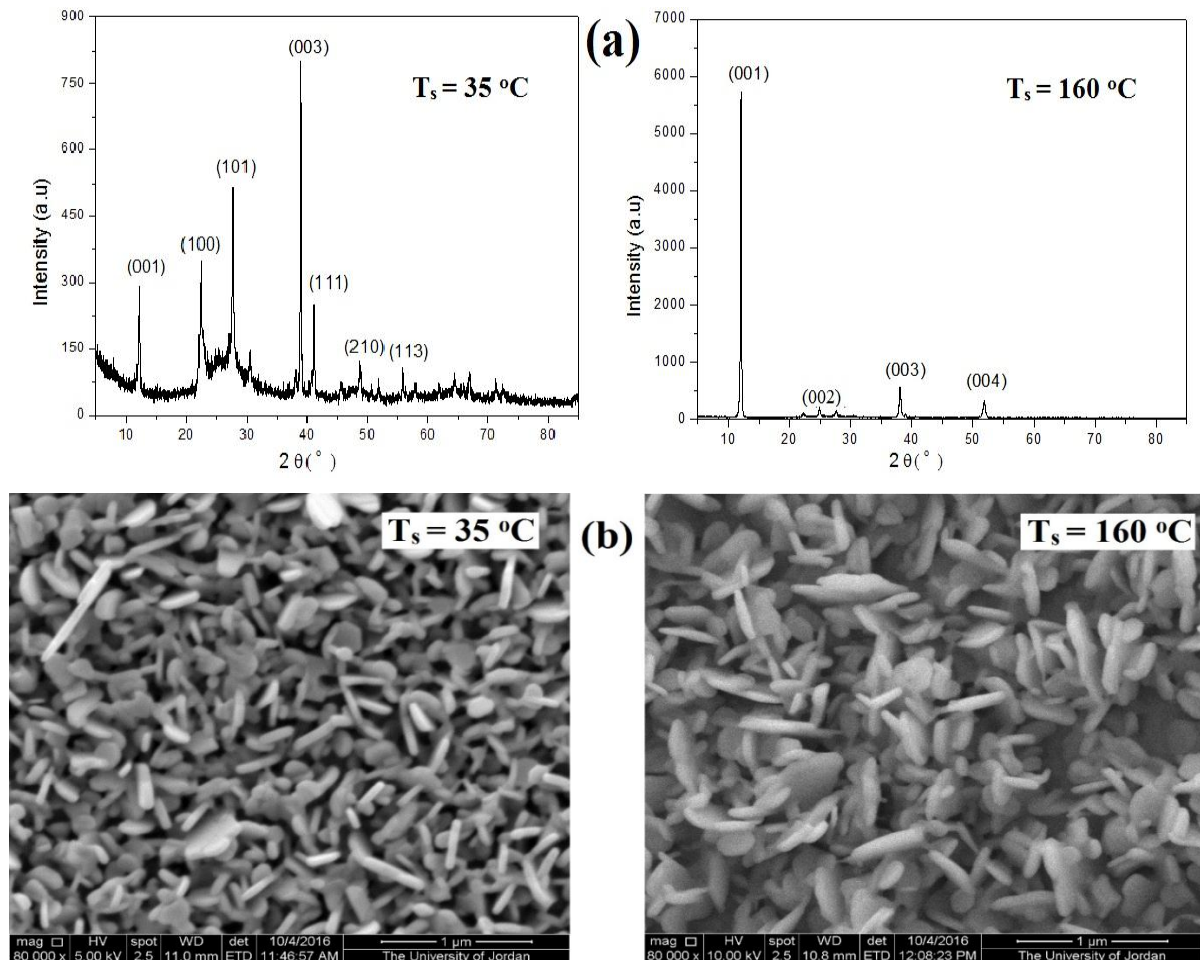


FIG. 1. (a) XRD pattern and (b) SEM micrograph for the 0.7- μm thick evaporated lead iodide film prepared at T_s (35 and 160 °C). (After permission from the author of Ref. [30]).

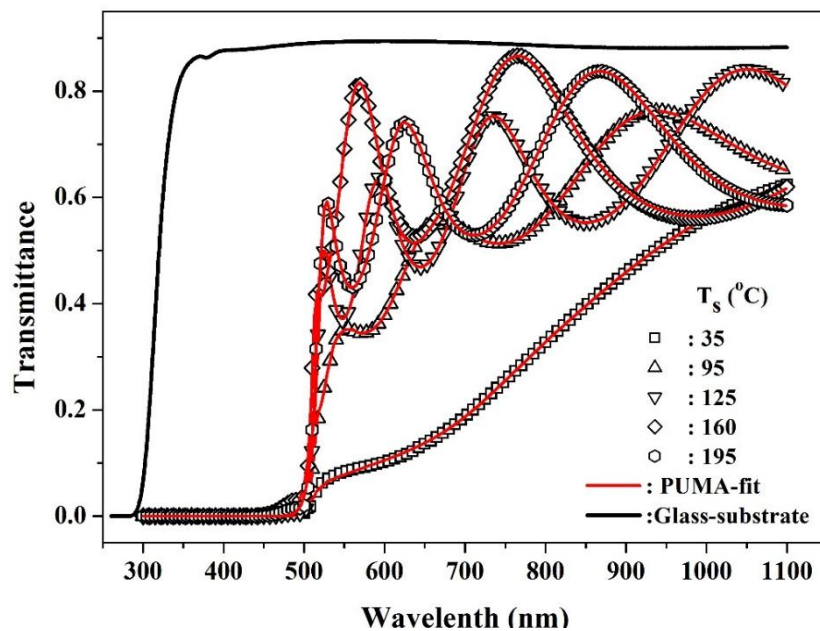


FIG. 2. As-measured normal-incidence $T_{\text{exp}}(\lambda) - \lambda$ spectra and their calculated PUMA-fit $T(\lambda) - \lambda$ curves for the thermally-evaporated PbI_2 films prepared at different substrate temperatures T_s (35-195 °C).

First, in the wavelength range 550-1100 nm, the $T_{\text{exp}}(\lambda) - \lambda$ curves of studied PbI_2 film/glass substrate samples exhibit high optical transmission that is characteristic of the weak/medium and transparent absorption regions of lead iodide. Their $T_{\text{exp}}(\lambda) - \lambda$ spectra at low substrate temperature < 100 °C were noted to be monotonic with variation of wavelength and no significant interference-fringe features have been observed; However, well resolved interference-fringes have been exhibited at higher T_s , suggesting that the lead iodide films deposited at high substrate temperatures become highly crystalline and relatively uniform in thickness. In the weak absorption and transparent regions of lead iodide films laid on glass substrates with extinction coefficients $\kappa(\lambda)$ and $\kappa_s(\lambda)$, the associated absorption coefficients $\alpha(\lambda) = 4\pi\kappa/\lambda$ and $\alpha_s(\lambda) = 4\pi\kappa_s/\lambda$ almost vanish and their $T_{\text{exp}}(\lambda) - \lambda$ spectra are just determined by their indices of refraction $n(\lambda)$ and $n_s(\lambda)$, where (s) designates the substrate material [14, 15].

Second, at a specific cut-off wavelength λ_c (≈ 520) nm and spectral wavelengths below, the measured $T_{\text{exp}}(\lambda) - \lambda$ curves of studied PbI_2 -films/glass substrate samples are seen to decline steadily towards zero transmittance, where λ_c represents the border of the absorption edge of the film material, which is for PbI_2 larger than that of soda-lime glass substrates ($\lambda_c \sim 350$ nm). In the strong absorption region ($\lambda < \lambda_c$) of lead iodide films, the transmission curves disappear of the (film/substrate) samples from the observed normal-incidence $T_{\text{exp}}(\lambda) - \lambda$ spectra and their transmission is exclusively determined by the absorption coefficient $\alpha(\lambda)$ of lead iodide films. This model approximation is helpful when discussing features of transmittance spectra of semiconducting films in the strong absorption region, where a drop in their transmission curves with decreasing wavelength occurs [16-19]. At $\lambda < \lambda_c$, absence of abrupt transmission of PbI_2 films prepared at low T_s can be accounted for by assuming that native and disorder structural imperfections (defects) and thickness non-uniformity are present in their thermally-evaporated PbI_2 films, which means lower crystallinity in comparison to the prepared films at high T_s that show clear interference-fringes and somewhat sharp dealing in $T_{\text{exp}}(\lambda)$.

Since $T(\lambda)$ is not an intrinsic property of the material, further analysis of the $T_{\text{exp}}(\lambda)$ data of air-supported PbI_2 -film/ glass-substrate samples by the PUMA method is needed to determine the dependency of their optical constants on the spectral wavelength λ or photon energy ($E = h\nu$) of the light incident onto them, where ν is its frequency and h is Planck's constant. The obtained results will then be used to elucidate the spectral dispersion of $n(\lambda)$ and $\kappa(\lambda)$ of PbI_2 films, besides exploiting the variation of their calculated absorption coefficient $\alpha(h\nu)$ with $h\nu$ to have further insight into the interband transitions responsible for optical absorption processes in these PbI_2 films. The PUMA method is an optical analysis that yields simulation curves that fit the measured spectra and retrieves optical constants $n(\lambda)$ and $\kappa(\lambda)$ of studied films as a function of wavelength λ [17]. This is in contrast to conventional curves fitting of experimental transmittance spectra of a multi-layered structure to a theoretical model that usually requires several suitable constant dispersion functions and must yield global solution of the problem to get true physically meaningful results. These problems are overcome by making use of the PUMA program to analyze normal-incidence transmittance of multi-layered structures, without prior need for dispersion relations [18, 19]. The PUMA software is free to download from the PUMA home page (<http://www.ime.usp.br/~egbirgin/puma>). The present optical analysis uses the PUMA program that characterizes the transmittance $T(\lambda)$ spectrum of single-film four-layered structures, with the numeric $n_s(\lambda)$ -formula of the film's substrate (assumed transparent $\kappa_s(\lambda) = 0$) given without any film dispersion relations being given. The PUMA program is pertinent, whether the measured transmittance spectra of such stacks exhibit interference fringes or not [17-19].

The PUMA program iteratively minimizes, *via specific ad hoc* procedure, the difference between $T_{\text{exp}}(\lambda)$ and calculated $T\{\lambda; n(\lambda), \kappa(\lambda)\}$ to get a solution, under a diversity of physical restrictions on the unknowns $n(\lambda)$ and $\kappa(\lambda)$ between the chosen minimum and maximum wavelengths λ that would lead to the equality $T_{\text{exp}}(\lambda) \cong T\{\lambda; n(\lambda), \kappa(\lambda)\}$ [18, 19].

Fig. 2 displays the correspondence between the measured normal-incidence $T_{\text{exp}}(\lambda) - \lambda$ spectra of the thermally-evaporated PbI_2 films studied in the present work and the simulated $T(\lambda) - \lambda$ curves that were recovered from the analysis of these $T_{\text{exp}}(\lambda) - \lambda$ spectra using the successive version of the PUMA program [17-19]. The transmittance curves retrieved from PUMA program profoundly simulate the measured transmittance spectra of such PbI_2 films over the entire spectral range studied.

Fig. 3 displays the variance of extinction coefficient $\kappa(\lambda)$ with λ of the PbI_2 films,

calculated using the results obtained from the analysis of $T_{\text{exp}}(\lambda)$ -spectra of their (film/substrate)-samples by the numeric PUMA method that employs the normal-incidence transmittance formulation [14-16, 18]. It can be noted from Fig. 3 that for $\lambda > 550$ nm, the values of $\kappa(\lambda)$ of studied PbI_2 films are (~ 0.02) almost negligible, but $\kappa(\lambda)$ starts to increase steadily with decreasing wavelength. The inset to Fig. 3 shows the $\alpha(h\nu) - h\nu$ plots for the PbI_2 films, where the absorption coefficient $\alpha(\lambda)$ was calculated from $\kappa(\lambda)$ using the relation

$$\alpha(\lambda) = 4\pi\kappa(\lambda)/\lambda. \quad (1)$$

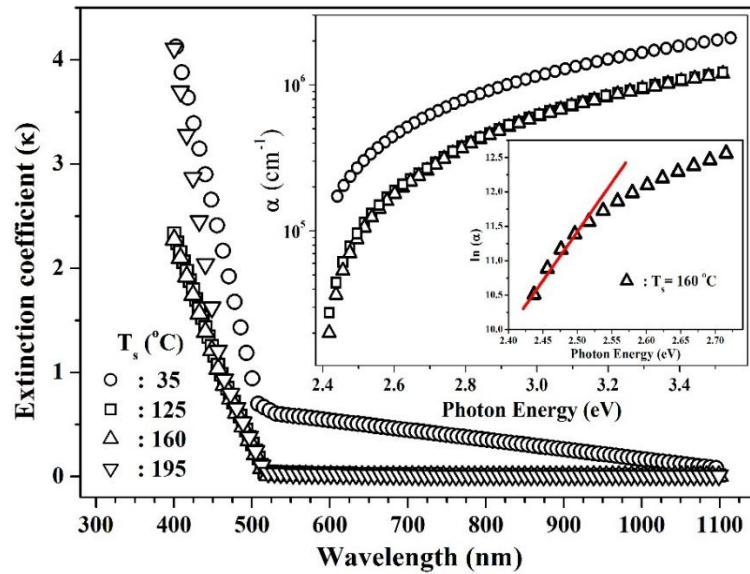


FIG. 3. Dispersion of extinction coefficient $\kappa(\lambda)$ of PbI_2 films retrieved from PUMA-analysis of their measured transmittance spectra. The inset shows the variation of absorption coefficient $\alpha(E)$ with photon energy E , depicting fits of low-energy $\alpha(E) - E$ data of the PbI_2 film prepared at ($T_s = 160$ °C) to Urbach exponential formula of Eq. (2).

The PUMA-retrieved dependency of $\alpha(h\nu)$ on $h\nu$ is nearly similar at high photon energies (> 2.5 eV). This can be related to band-gap absorption being affected by localized energy states in the band gap (Urbach-tails) due to some disorder and native defects in PbI_2 films [13]. Analysis of low energy part of $\alpha(h\nu) - h\nu$ data close to the absorption edge of a semiconductor, in view of the Urbach formula given below in Eq. (2), is assumed to give small but physically significant values for the range of bandgap tails (Urbach-tail breadth Γ_U) [13, 17, 34, 35].

$$\alpha(h\nu) = \alpha_o \exp[(h\nu - E_{0U})/\Gamma_U] \quad (2)$$

where Γ_U is the Urbach energy equal to the energy width of the absorption-edge tail which can be calculated from the relation $\Gamma_U^{-1} = \Delta(\ln \alpha)/\Delta(h\nu)$ and α_o and E_{0U} are the

coordinates of the convergence point of the Urbach “bundle” [34]. For the ($\text{PbI}_2/\text{glass}$)-samples of this work, the analysis result of PUMA-calculated $\alpha(h\nu)$ data in the (Urbach-tail) part is plotted in the inset of Fig. 3 as a $\ln[\alpha(h\nu)]$ plot for the PbI_2 film prepared at $T_s = 160$ °C. The slopes, derived from fits of low-energy linear parts of $\ln[\alpha(h\nu)] - h\nu$ plots, give the Urbach-tail breadths Γ_U for studied PbI_2 films and are listed in Table 2. The values of Urbach-tail parameter Γ_U for the films prepared at 35 °C were relatively high, but at high substrate temperatures, these values were around (70 – 80 meV) and are in agreement with those reported by Ghosh [23]. It is noted from Table 2, that the values of Γ_U decreased with increasing T_s , indicating that with increasing T_s at which the PbI_2 films were prepared, their crystallinity was

enhanced as the disorder lattice become less effective.

To investigate the properties of band-to-band optical absorption in a semiconducting film, the change of its absorption coefficient at the edge of optical absorption region of the material is usually exploited as a function of the incident photon energy $h\nu$. Several theoretical and experimental approaches have tackled the phenomenon of optical absorption in semiconductors [36]. The approximate formulations generally adopted to describe the behavior of the absorption coefficient $\alpha(h\nu)$ in semiconductors in their interband transition regions have been employed in this work using the $\alpha(h\nu) - h\nu$ data calculated from the PUMA-analysis of $T_{\text{exp}}(\lambda)$ spectra of (PbI₂/glass) samples. Various optical absorption models, both the direct and indirect interband transition models, are often described by Eq. (3) and have been commonly adopted to clarify the mechanism of optical absorption in the absorption-edge region [13, 17, 36-38], viz.

$$\alpha h\nu = A (h\nu - E_g)^m \quad (3)$$

where A is a constant of the sample material that is almost independent of the photon energy. For allowed indirect and direct band-to-band transitions, $m = 2$ and $m = 1/2$, respectively. As lead iodide is usually considered to be a

direct-band p -type semiconductor compound, the $\alpha(h\nu) - h\nu$ formula being used in this work is that which allows direct band-to-band electronic transitions; namely, $(\alpha h\nu)^2 = A(h\nu - E_g)$ [12, 21-29]. The direct and indirect interband transition models were these treated in detail and employed to analyze PUMA-retrieved $\alpha(h\nu) - h\nu$ data of PbI₂ films studied in this work by presenting this data on $[\alpha h\nu]^{1/2} - h\nu$ and $[\alpha h\nu]^2 - h\nu$ plots as seen in Fig. 4 for typical (PbI₂/glass) samples. It was found that intersections (bandgap energy) of linear portions of these plots with $h\nu$ -axis, deduced from curve-fits of the $\alpha(h\nu) - h\nu$ data to Tauc (indirect) law $\{\alpha h\nu \propto (h\nu - E_g^{\text{opt}})^2\}$ and to the direct interband-transition relation $\{\alpha h\nu \propto (\sqrt{h\nu - E_g})\}$, do not match with each other. Figure 4 depicts curve-fits of PUMA-retrieved $\alpha(h\nu) - h\nu$ data of PbI₂ films to the Tauc formulae and direct interband transition models, with the Tauc optical bandgap energy E_g^{opt} and the direct bandgap energy E_g around 2.2 eV and 2.45 eV, respectively (see Table 2). The values of E_g (~ 2.5 eV) for the PbI₂ films studied in this work agree with the results of the direct energy gap calculated from other studies on PbI₂ films [12, 21-29]. Some studies [12, 22, 26-29] found that the direct E_g decreases as the film thickness increases.

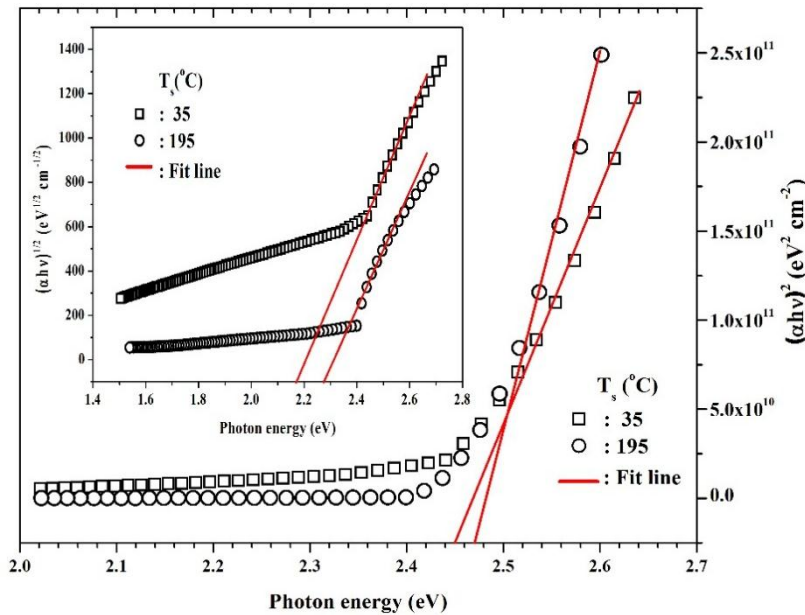


FIG. 4. PUMA-retrieved $\alpha(h\nu) - h\nu$ data of PbI₂ films on $(\alpha h\nu)^2 - h\nu$ and least-square fits (lines) of linear portions on such plots for the PbI₂ films prepared at T_s (35 and 195 °C). Inset depicts $\sqrt{\alpha h\nu} - h\nu$ (Tauc-law) plots.

There is some controversy over the origin and properties of interband optical absorption in lead iodide and hence on the real value of bandgap energy, which has been obtained from the direct interband transition model [12, 21-29]. Analysis of $\alpha(h\nu) - h\nu$ data of PbI_2 films showed that optical absorption in PbI_2 films can be described by the indirect interband transition model over a narrow range of photon energies, but can be represented by the direct interband transition model on the basis of the $(\alpha h\nu)^2 \propto (h\nu - E_g)$ formula over a broader spectral range in the strong absorption-edge region, over which this direct formulation has been discussed by other researchers to give the best fit of the $\alpha(h\nu) - h\nu$ data of their PbI_2 films [12, 21-29]. The quality and crystallinity of the prepared PbI_2 films seem to be the reason behind the diversity of the determined values of bandgap energy of PbI_2 , in addition to the use of different interband and sub-bandgap transition models to exploit its optical absorption phenomenon. Nonetheless, such diversity in the values of the bandgap

energy of PbI_2 that were deduced based on different absorption models critically depends on which data points are selected to be curve-fitted to a linear portion on the $(\alpha h\nu)^{1/m} - (h\nu - E_g)$ plots.

The quality of PbI_2 films and their performance were integrated in optical/electronic devices and this can be exploited from studying their index of refraction $n(\lambda)$ and optical dispersion. Fig. 5 shows the wavelength dispersion of the index of refraction $n(\lambda)$ of the PbI_2 films of the present work. The $n(\lambda) - \lambda$ data has been obtained from the analysis of the ($\text{PbI}_2/\text{glass-substrate}$) samples using the numeric PUMA program [14, 18]. For $\lambda > 550$ nm, the values of $n(\lambda)$ are nearly the same for studied films, pointing that PUMA method works acceptably well for comparatively thick films and PbI_2 films had no major divergence in their properties, implying that their fabrication procedures were alike.

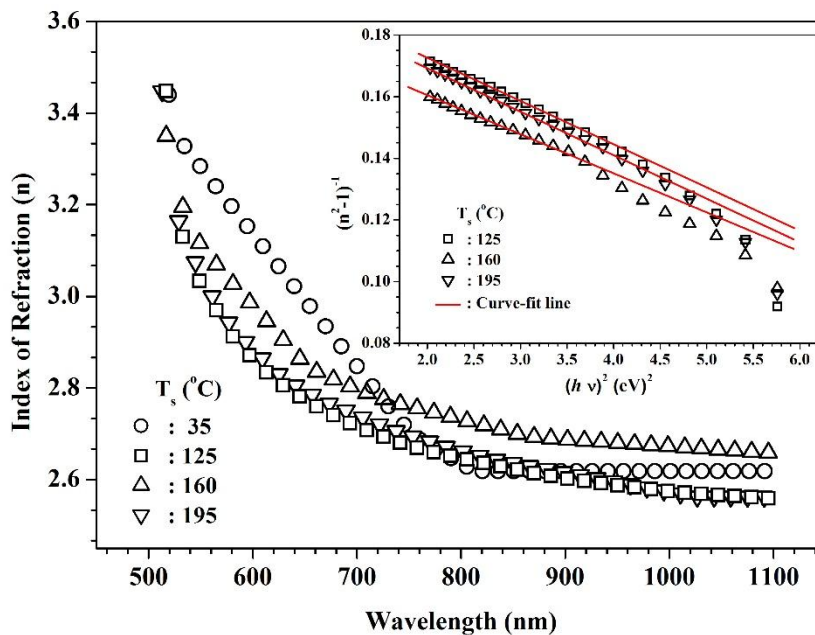


FIG. 5 Spectral dispersion of index of refraction $n(\lambda)$ of PbI_2 films determined from PUMA analysis of $T_{\text{exp}}(\lambda)$ spectra of their samples. The inset depicts curve-fits of low photon-energy PUMA-retrieved $\{[n(E)]^2 - 1\}^{-1} - E^2$ data of PbI_2 films to the Wemple-DiDomenico dispersion formula: Eq. (4).

The change of $n(\lambda)$ of a film in its optical transparency and absorption ranges with λ can be analyzed using the Wemple-DiDomenico (WDD) $n(E) - E$ dispersion formula, which is expressed in terms of photon energy $E_{\text{ph}} (= h\nu)$ of the light beam striking the film in the relation [40]:

$$[n(h\nu)]^2 = 1 + \frac{E_0 E_d}{E_0^2 - (h\nu)^2} \quad (4)$$

The WDD formula includes two constant parameters, which are related to the physical properties of the material: the single-oscillator energy parameter E_0 , related to the Tauc optical bandgap energy as $E_0 \cong 2E_g^{\text{opt}}$ [36, 40] and the

Using the PUMA Method

single-oscillator energy strength E_d . Using the PUMA-retrieved $n(\lambda)$ data, the variation of $n(\lambda)$ with $h\nu$ was achieved by plotting $\{[n(h\nu)]^2 - 1\}^{-1} - V_s - (h\nu)^2$ as seen in the inset to Fig. 5, where the intercept ($= E_o/E_d$) of a linear part at $h\nu = 0$ and slope ($= -1/E_d E_o$) can be used to calculate the static index of refraction $n_o = \sqrt{1 + E_d/E_o}$ [40]. The obtained values of E_o , E_d

and n_o for thermally-evaporated PbI_2 films in this work are listed in Table 2. This shows that the optical analysis founded on the PUMA method is successful in our spectral range and shows that for $T_s > 100$ °C, the bandgap energy parameter $E_o \cong 3.9$ eV, single-oscillator energy strength $E_d \cong 19$ eV and static index of refraction $n_o \cong 2.5$.

TABLE 2. The PUMA-retrieved data of PbI_2 films and fit parameters found from curve-fits of their PUMA-retrieved $n(\lambda) - \lambda$ data to Wemple-DiDomenico (WDD) dispersion formula, $\alpha(h\nu) - h\nu$ data to Tauc and direct interband transition models and to Urbach-tail formula.

Method of analyzing optical constants		Sample	S35	S95	S125	S160	S195
fit parameter							
WDD $n(E)$ -formula, Eq. (4)		E_d (eV)	24.9	15.4	19.9	18.3	19.1
		E_o (eV)	3.87	3.98	3.93	3.53	3.77
		n_o	2.72	2.2	2.46	2.48	2.46
Urbach-tail rule, Eq. (2)		Γ_U (meV)	150	89.6	71.5	75.9	79.6
Interband transition model, Eq. (3)	Direct ($m = 1/2$)	E_g (eV)	2.45	2.44	2.45	2.47	2.47
	Tauc ($m = 2$)	E_g^{opt} (eV)	2.18	2.16	2.23	2.25	2.26

Conclusions

The normal-incidence transmittance $T_{\text{exp}}(\lambda)$ of $0.7 - \mu\text{m}$ thick PbI_2 films deposited on 1.1-mm thick glass slides maintained at different substrate temperatures ($35 - 195$ °C) has been measured at room temperature as a function of the spectral wavelength λ in the UV-VIS-NIR region ($\lambda = 300 - 1100$ nm).

The values of E_g^{opt} and E_g of the studied PbI_2 films, determined from the analysis of the calculated $\alpha(h\nu) - h\nu$ data using the indirect (Tauc) and direct interband transition models, were found to be around 2.2 eV and 2.45 eV, respectively, for all samples regardless of substrate temperatures, while the values of the Urbach-tail parameter Γ_U , deduced from the analysis of the PUMA-retrieved $\alpha(h\nu) - h\nu$ data belonging to the sub-bandgap transition region based on the Urbach exponential law, were found to be around ($70 - 80$ meV) at substrate temperatures $T_s > 100$ °C, below which the values of Γ_U were lower, indicating some band-tailing in the bandgap that has been reduced upon crystallinity improvement. The refractive index $n(\lambda)$ of studied PbI_2 films was found to vary with λ markedly with spectral wavelength nearby the absorption edge of PbI_2 and was well described by the Wemple-DiDomenico formula, the least-square fit curves of which gave comparable static index of refraction $n_o \cong 2.5$ for films prepared at $T_s > 100$ °C. The single-

oscillator energy parameter $E_o \cong 3.9$ eV $\cong 2 E_g^{\text{opt}}$. The Tauc optical bandgap energy results are in good agreement with theoretical predictions. The analysis of the WDD formulation gave nearly the same single-oscillator energy strength E_d (~ 19 eV) for highly crystalline films as for those PbI_2 films prepared at substrate temperatures above 100 °C.

As the stoichiometry of prepared thermally-evaporated lead iodide films was not good, further understanding of the optical response of PbI_2 films and associated energy band structure may be achieved if accurate transmittance/reflectance measurements are made on crystalline PbI_2 films deposited on transparent substrates by other fabrication methods, such as flash-evaporation technique, over a broader spectral range ($300 - 700$ nm). Simulation of the measured transmittance spectra using modified versions of the PUMA program that can handle optical data of thick/thin films and that consider dispersion and optical absorption in their substrates is also appealing. Furthermore, the application of normal-incidence transmission envelope theories to both uniform and non-uniform PbI_2 films prepared by different methods whose optical spectra exhibit many interference-fringe maxima and minima, armed with reliable transmission envelopes, will be complementary.

Acknowledgements

My deepest appreciation goes to Prof. Mousa M. Abdul-Gader Jafar, for his profound insight, continuous support and wise guidance. His

priceless suggestions enhanced the standard of the work considerably.

References

- [1] Moy, J.P., Nucl. Instr. and Meth. A, 442 (2000) 26.
- [2] Hassan, M.A. and Jafar, M.M.A., Nucl. Instr. and Meth. A, 566 (2006) 526.
- [3] Hensch, H.K. and Srinivasagopalan, C., Solid State Communication, 4 (1966) 415.
- [4] Deich, V. and Roth, M., Nucl. Instr. and Meth. A, 380 (1996) 169.
- [5] Lund, J.C., Shah, K.S., Squillante, M.R., Moy, L.P., Sinclair, F. and Entine, G., Nucl. Instr. and Meth. A, 283 (1989) 299.
- [6] Minder, R., Ottaviani, G. and Canali, C., J. Phys. Chem. Solids, 37 (1976) 417.
- [7] Shah, K.S., Street, R.A., Dmitriyev, Y., Bennett, P., Cirignano, L., Klugerman, M., Squillante, M. R. and Entine, G., Nucl. Instr. and Meth. A, 458 (2001) 140.
- [8] Schieber, M., Lund, J.C., Olsen, R.W., McGregor, D.C., Van Scyoc, J.M., James, R.B., Soria, E. and Bauser, E., Nucl. Instr. and Meth. A, 377 (1996) 492.
- [9] Lund, J.C., Olschner, F. and Burger, A., Semiconductors and Semimetals, 43 (1995) 443.
- [10] Ahuja, R., Arwin, H., Ferreira da Silva, A., Persson, C., Osorio-Guillen, J.M., Souza de Almeida, J., Moyses Araujo, C., Veje, E., Veissid, N., An, C.Y., Pepe, I. and Johansson, B., Journal of Applied Physics, 92 (2002) 7219.
- [11] Matuchova, M., Zdansky, K., Zavadil, J., Tonn, J., Jafar, M.M.A-G., Danilewsky, A.N., Cröll, A. and Maixner, J., Journal of Crystal Growth, 312 (2010) 1233.
- [12] Bhavsar, D.S. and Saraf, K.B., J. Mater. Sci.: Mater. Electron., 14 (2003) 195.
- [13] Saleh, M.H., Jafar, M.M.A-G., Bulos, B.N. and Al-Daraghme, T.M.F., Appl. Phys. Res., 6 (2014) 10.
- [14] Swanepoel, R., J. Phys. E: Sci. Instrum., 16 (1983) 1214.
- [15] Saleh, M.H., Ershaidat, N.M., Ahmad, M.J.A., Bulos, B.N. and Jafar, M.M.A-G., Opt. Rev., 24 (2017) 260.
- [16] Jafar, M.M.A-G., European Int. J. Sci. Technol., 2 (2013) 274.
- [17] Jafar M.M.A-G., Saleh, M.H., Ahmed, M.J.A., Bulos, B.N. and Al-Daraghme, T.M., J. Mater. Sci.: Mater. Electron., 27 (2016) 3281.
- [18] Birgin, E.G., Chambouleyron, I. and Martinez, J. Comp. Phys., 151 (1999) 862.
- [19] Mulato, M., Chambouleyron, E.G., Birgin, J.M. and Martínez, Appl. Phys. Lett., 77 (2000) 2133.
- [20] Condeles, J.F., Lofrano, R.C.Z., Rosolen, J.M. and Mulato, M., Brazilian Journal of Physics, 36 (2006) 320.
- [21] Saleh, M.H., Ph.D. Thesis, University of Jordan, (2011), Jordan.
- [22] Shkir, M., Abbas H. and Khan, Z.R., Journal of Physics and Chemistry of Solids, 73 (2012) 1309.
- [23] Ghosh, T., Bandyopadhyay, S., Roy, K.K., Kar, S., Lahiri, A.K., Maiti, A.K. and Goswami, K., Cryst. Res. Technol., 43 (2008) 959.
- [24] Kariper, I.A., Opt. Rev., 23 (2016) 401.
- [25] Jamil, S.S., Mousa, A.M., Mohammad, M.A. and Thajeel, K.M., Eng. & Tech. Journal, 29 (2011) 531.
- [26] Acuna, D., Krishnan, B., Shaji, S., Sepulveda, S. and Menchaca, J.L., Bull. Mater. Sci., 39 (2016) 1453.
- [27] Kumar, S. and Sharma, S., International Journal of Engineering Research & Technology, 2 (2013) 3593.

- [28] Agrawal, H., Vedeshwar, A.G. and Saraswat, V.K., *Journal of Nano Research*, 24 (2013) 1.
- [29] Bhavsar, D.S., *Advances in Applied Science Research*, 2 (2011) 92.
- [30] Shehadeh, K.M., M.Sc. Thesis, The University of Jordan, (2017), Jordan.
- [31] Al-Daraghme, T.M., Saleh, M.H., Ahmad, M.J.A., Bulos, B.N., Shehadeh, K.M. and Jafar, M.M.A-G., *Journal of Electronic Materials*, 47 (2018) 1806.
- [32] Schieber, M., Zamoshchik, N., Khakhan, O. and Zuck, A., *Journal of Crystal Growth*, 310 (2008) 3168.
- [33] Dmitriev, Y., Bennett, R.B., Cirignano, L.J., Klugerman, M. and Shah, K.S., *Nucl. Instr. and Meth. A*, 592 (2008) 334.
- [34] Studenyak, I., Kranjčec, M. and Kurik, M., *International Journal of Optics and Applications*, 4 (3) (2014) 76.
- [35] O'Leary, S.K., Johnson, S.R. and Lim, P.K., *J. Appl. Phys.*, 82 (1997) 3334.
- [36] Tan, W.C., Koughia, K., Singh, J. and Kasap, S.O., "Optical Properties of Condensed Matter and Applications", Ed. J. Singh, (John Wiley, London, 2006), Chapter 1.
- [37] Tauc, J., "Optical Properties of Solids", Ed. F. Abelés (North-Holland, Amsterdam, 1972), pp. 277-310.
- [38] Dragoman, D. and Dragoman, M., "Optical Characterization of Solids", (Springer-Verlag, Berlin, 2002).
- [39] Mott, N.F. and Davis, E.A., "Electronic Processes in Non-Crystalline Materials", 2nd Ed. (Clarendon Press, Oxford, 1979).
- [40] Wemple, S.H. and DiDomenico, M., *Phys. Rev. B*, 3 (1971) 1338.